Supporting Information.

Highly efficient benzyl alcohol valorisation via the in-situ synthesis of H_2O_2 and associated reactive oxygen species.

Gregory Sharp[a†], Richard J. Lewis[a†*], G. Magri[b], J. Liu[c], David J. Morgan[a,d], Thomas E. Davies[a], , Ángeles López-Martín[a], Damien M. Murphy[b], Andrea Folli[e] Liwei Chen[c], Xi Liu[c,f*] and Graham J. Hutchings[a*]

[a]Max Planck-Cardiff Centre on the Fundamentals of Heterogeneous Catalysis FUNCAT, Cardiff Catalysis Institute, School of Chemistry, Cardiff University, Translational Research Hub, Maindy Road, Cardiff, CF24 4HQ, United Kingdom.

[b]School of Chemistry, Cardiff University, Main Building, Park Place, Cardiff, CF10 3AT, United Kingdom.

[c]In-situ Centre for Physical Sciences, School of Chemistry and Chemical, Frontiers Science Centre for Transformative Molecules, Shanghai 200240, P. R. China

[d]HarwellXPS, Research Complex at Harwell (RCaH), Didcot, OX11 OFA, United Kingdom.

[e]Net Zero Innovation Institute, Cardiff Catalysis Institute, School of Chemistry, Cardiff University, Translational Research Hub, Maindy Road, Cardiff, CF24 4HF, United Kingdom.

[f]School of Chemistry and Chemical Engineering, Ningxia University, Yinchuan 750021, P. R. China

[†]These authors contributed equally to this work.

*LewisR27@Cardiff.ac.uk, LiuXi@stju.edu.cn, Hutch@Cardiff.ac.uk

Table S.1. The surface area of 0.5%Au-0.5%Pd/X catalysts, as a function of catalyst support, as determined by BET.

Catalyst	Surface Area / m^2g^{-1}
0.5%Au-0.5%Pd/Al_2O_3	74
γ-Al_2O_3	83
0.5%Au-0.5%Pd/CeO_2	43
CeO_2	36
0.5%Au-0.5%Pd/TiO_2	42
TiO_2 (P25)	53
0.5%Au-0.5%Pd/Nb_2O_5	8
Nb_2O_5	8
0.5%Au-0.5%Pd/ZrO_2	9
ZrO_2	21

Note: Surface area determined from nitrogen adsorption measurements using the BET equation. Support material used as received, with no modification prior to metal immobilisation. Catalytic samples exposed to a reductive heat treatment (5%H_2/Ar, 500 ^oC, 4 h, 10^oC min^{-1}).

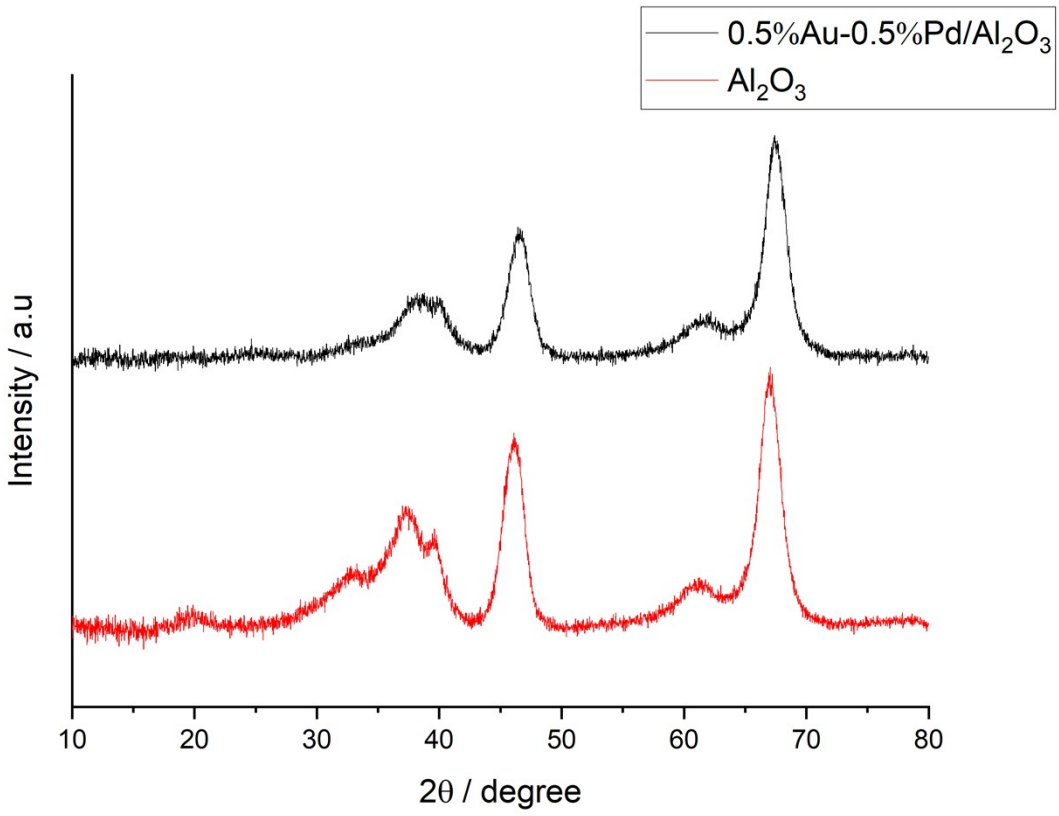

Figure S.1.A X-ray diffractogram of the 0.5%Au-0.5%Pd/Al_2O_3 catalyst, prepared by a wet co-impregnation methodology. **Note**: Catalyst exposed to a reductive heat treatment (5%H_2/Ar, 4 h, 500 °C, 10 °Cmin^{-1}). Support material used as received.

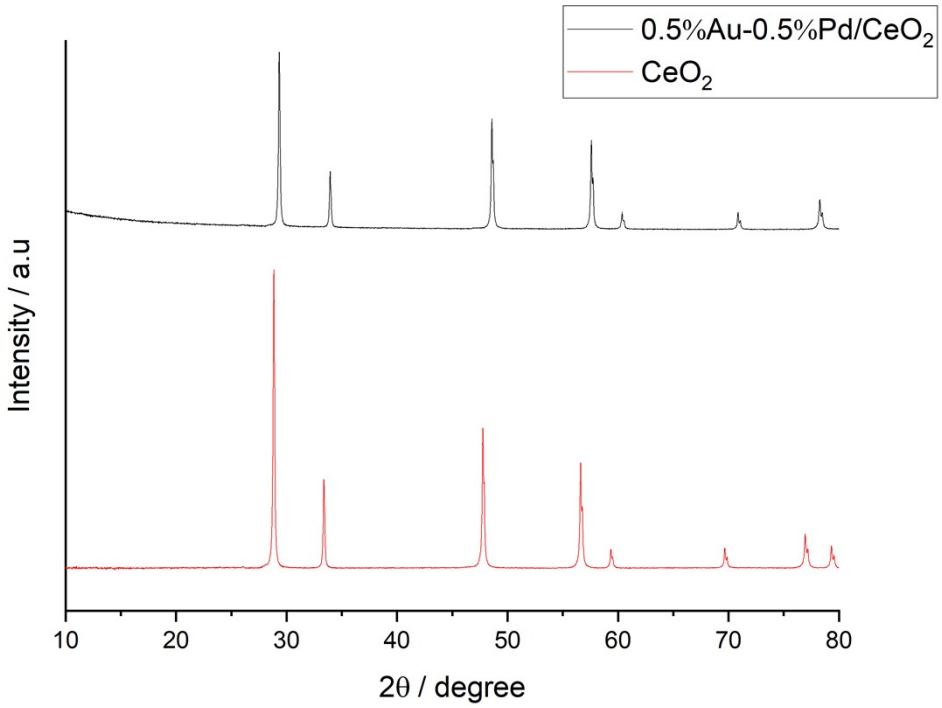

Figure S.1.B. X-ray diffractogram of the 0.5%Au-0.5%Pd/CeO_2 catalyst, prepared by a wet co-impregnation methodology. **Note**: Catalyst exposed to a reductive heat treatment (5%H_2/Ar, 4 h, 500

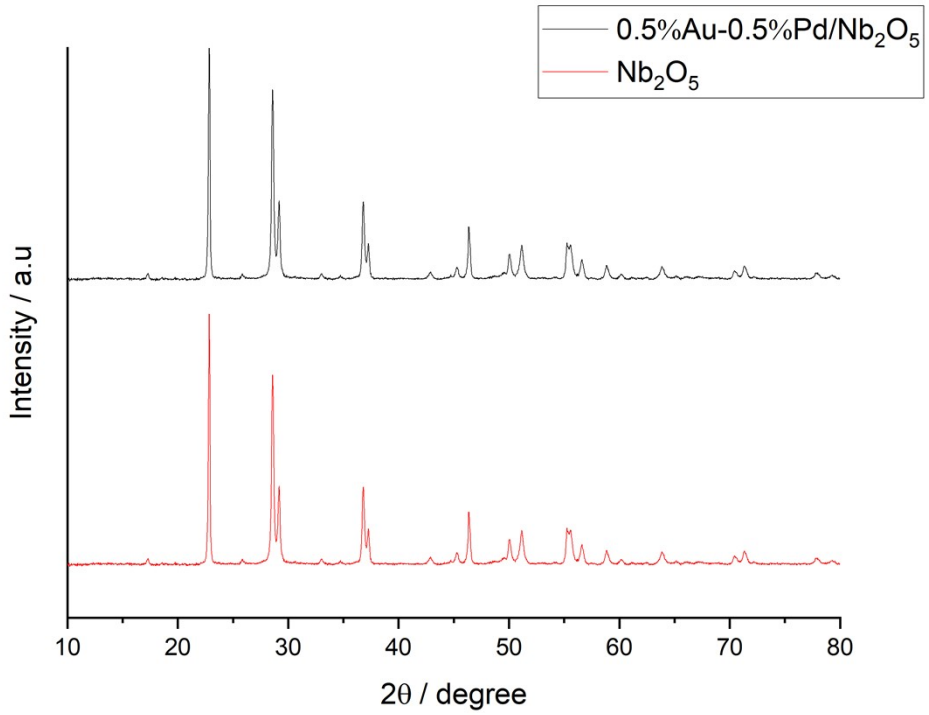

°C, 10 °Cmin^{-1}). Support material used as received.

Figure S.1.C. X-ray diffractogram of the 0.5%Au-0.5%Pd/Nb_2O_5 catalyst, prepared by a wet co-impregnation methodology. **Note**: Catalyst exposed to a reductive heat treatment (5%H_2/Ar, 4 h, 500 °C, 10 °Cmin^{-1}). Support material used as received.

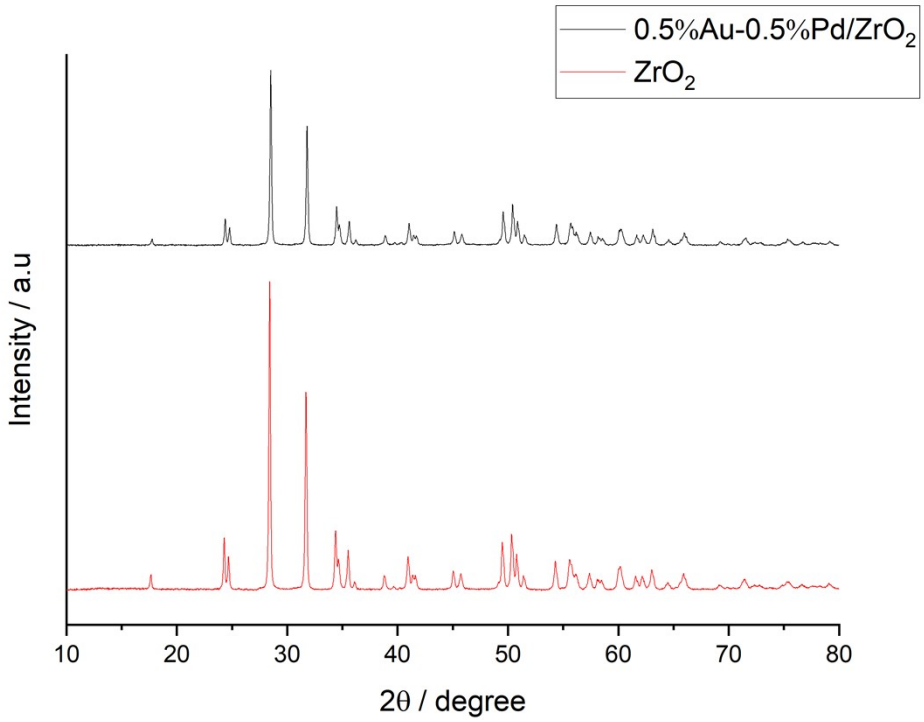

Figure S.1.D. X-ray diffractogram of the 0.5%Au-0.5%Pd/ZrO_2 catalyst, prepared by a wet co-impregnation methodology. **Note**: Catalyst exposed to a reductive heat treatment (5%H_2/Ar, 4 h, 500 °C, 10 °Cmin^{-1}). Support material used as received.

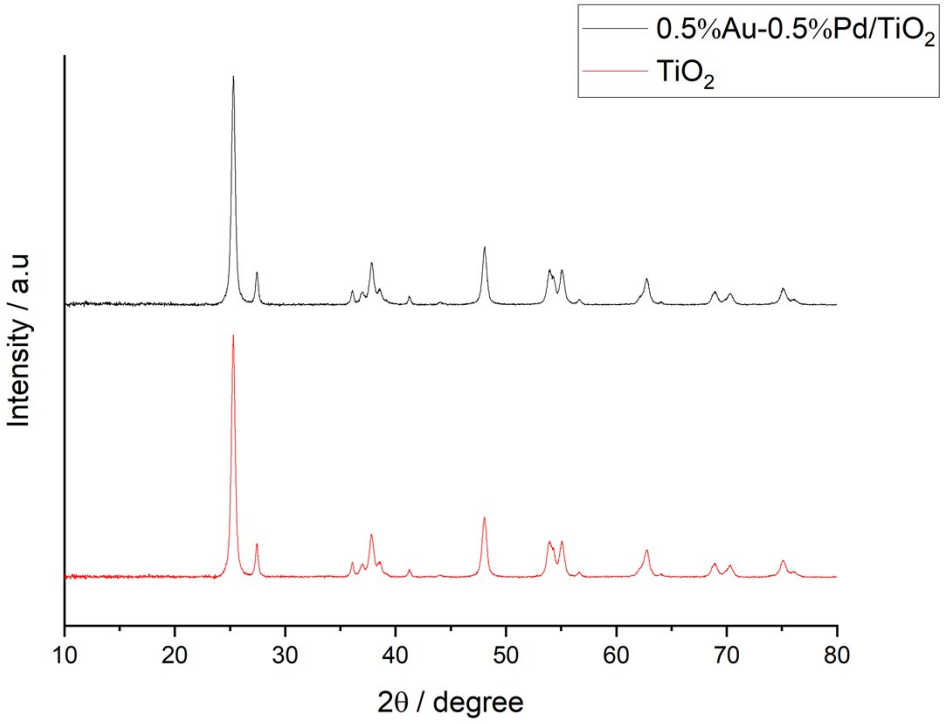

Figure S.1.E. X-ray diffractogram of the 0.5%Au-0.5%Pd/TiO_2 catalyst, prepared by a wet co-impregnation methodology. **Note**: Catalyst exposed to a reductive heat treatment (5%H_2/Ar, 4 h, 500 °C, 10 °Cmin^{-1}). Support material used as received.

Table S.2.A. Actual metal loading of supported AuPd catalysts, as a function of catalyst support, as determined by ICP-MS microwave-assisted aqua-regia digestion.

Catalyst	Actual loading / wt.%	
	Au	Pd
0.5%Au-0.5%Pd/Al_2O_3	0.48	0.49
0.5%Au-0.5%Pd/CeO_2	0.46	0.47
0.5%Au-0.5%Pd/TiO_2	0.49	0.50
0.5%Au-0.5%Pd/Nb_2O_5	0.45	0.48
0.5%Au-0.5%Pd/ZrO_2	0.47	0.49

Note: Digestion and analysis carried out on as-prepared dried catalysts.

Table S.2.B. Actual metal loading of 1%AuPd/Al_2O_3 catalysts, as a function of Au: Pd ratio, as determined by ICP-MS microwave-assisted aqua-regia digestion.

Catalyst	Actual loading / wt.%	
	Au	Pd
1%Au/Al_2O_3	0.98	-
0.75%Au-0.25%Pd/Al_2O_3	0.75	0.23
0.5%Au-0.5%Pd/Al_2O_3	0.48	0.49
0.25%Au-0.75%Pd/Al_2O_3	0.23	0.74
1%Pd/Al_2O_3	-	0.99

Note: Digestion and analysis carried out on as-prepared dried catalysts.

Table S.3. Activity of AuPd catalysts towards the oxidation of benzyl alcohol via in-situ H_2O_2 synthesis, as a function of catalyst support.

Catalyst	Benzyl alcohol Conv. / %	Benzaldehyde Sel. / %	Benzoic acid Sel. / %	H_2 Conv. / %	H_2 Sel. / %	Residual H_2O_2 / wt.%
0.5%Au-0.5%Pd/Al_2O_3	22.7	98.2	1.8	71	76	0.04
0.5%Au-0.5%Pd/CeO_2	2.7	100	0	12	55	0.03
0.5%Au-0.5%Pd/TiO_2	3.0	100	0	71	10	0.04
0.5%Au-0.5%Pd/Nb_2O_5	0.4	100	0	10	9	0.4
0.5%Au-0.5%Pd/ZrO_2	1.2	100	0	8	35	0.03

In-situ oxidation of benzyl alcohol reaction conditions: Catalyst (0.01 g), benzyl alcohol (1.04 g, 9.62 mmol), MeOH (7.1 g), 5%H_2/CO_2 (420 psi), 25%O_2/CO_2 (160 psi), 50 °C, 0.5 h, 1200 rpm. **Note:** H_2 selectivity determined, based on the mol of H_2 utilised in the formation of benzaldehyde.

Table S.4. Activity of AuPd catalysts towards the oxidation of benzyl alcohol via in-situ H_2O_2 synthesis, as a function of catalyst support.

Catalyst	Benzyl alcohol Conv. / %	Benzaldehyde Sel. / %	Benzoic acid Sel. / %	H_2 Conv. / %	H_2 Sel. / %	Residual H_2O_2 / wt.%
1%Au/Al_2O_3	0	0	0	B.D.L	-	0
0.75%Au-0.25%Pd/Al_2O_3	6.6	100	0	49	33	0.07
0.5%Au-0.5%Pd/Al_2O_3	22.7	98.2	1.8	71	76	0.04
0.25%Au-0.75%Pd/Al_2O_3	25.5	98.8	1.2	76	81	0.03
1%Pd/Al_2O_3	16.7	100	0	65	63	0.12
0.5%Pd/Al_2O_3	12.6	100	0	46	67	0.10

In-situ oxidation of benzyl alcohol reaction conditions: Catalyst (0.01 g), benzyl alcohol (1.04 g, 9.62 mmol), MeOH (7.1 g), 5%H_2/CO_2 (420 psi), 25%O_2/CO_2 (160 psi), 50 °C, 0.5 h, 1200 rpm. **Note:** H_2 selectivity determined, based on the mol of H_2 utilised in the formation of benzaldehyde. **B.D.L.:** Below detection limit.

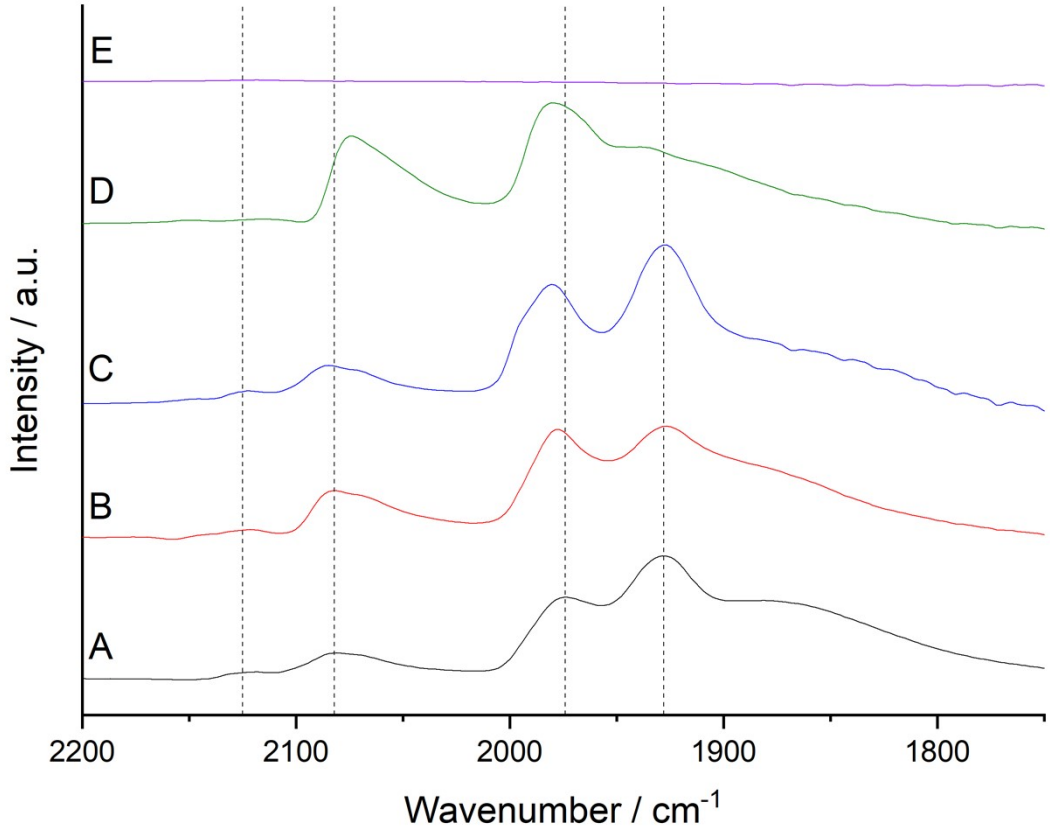

Figure S.2. CO-DRIFTS spectra for 1%AuPd/Al_2O_3 catalysts as a function of Au: Pd ratio. **(A)** 1%Pd/Al_2O_3 **(B)** 0.25%Au-0.75%Pd/Al_2O_3 **(C)** 0.5%Au-0.5%Pd/Al_2O_3 **(D)** 0.75%Au-0.25%Pd/Al_2O_3 **(E)** 1%Au/Al_2O_3. **Note**: All catalysts exposed to a reductive heat treatment (5%H_2/Ar, 4 h, 500 °C, 10 °Cmin^{-1}).

Supplementary Note for Figure S.2.

With the exception of the 1%Au/Al_2O_3 formulation, the CO-DRIFTS spectra of the AuPd catalysts can be seen to be dominated by Pd–CO bands. In the case of the monometallic Au the lack of an observable signal is attributed to the transient nature of the Au-CO interaction at ambient temperature. It is possible to attribute the peaks within the lower wavenumber region of the spectra (approx. 2000-1800 cm^{-1}) to the multi-fold adsorption of CO on extended Pd domains (i.e., CO adsorbed in a bidentate or tridentate manner), while those within the higher wavenumber region of the spectra (> 2000 cm^{-1}) are attributed to CO linearly adsorbed to low coordination Pd sites (i.e., edges or corners). Upon the alloying of Pd with Au a general blueshift, towards higher wavenumbers, was observed in both regions, which can be related to the transfer of electron density from Au to Pd.[1, 2]

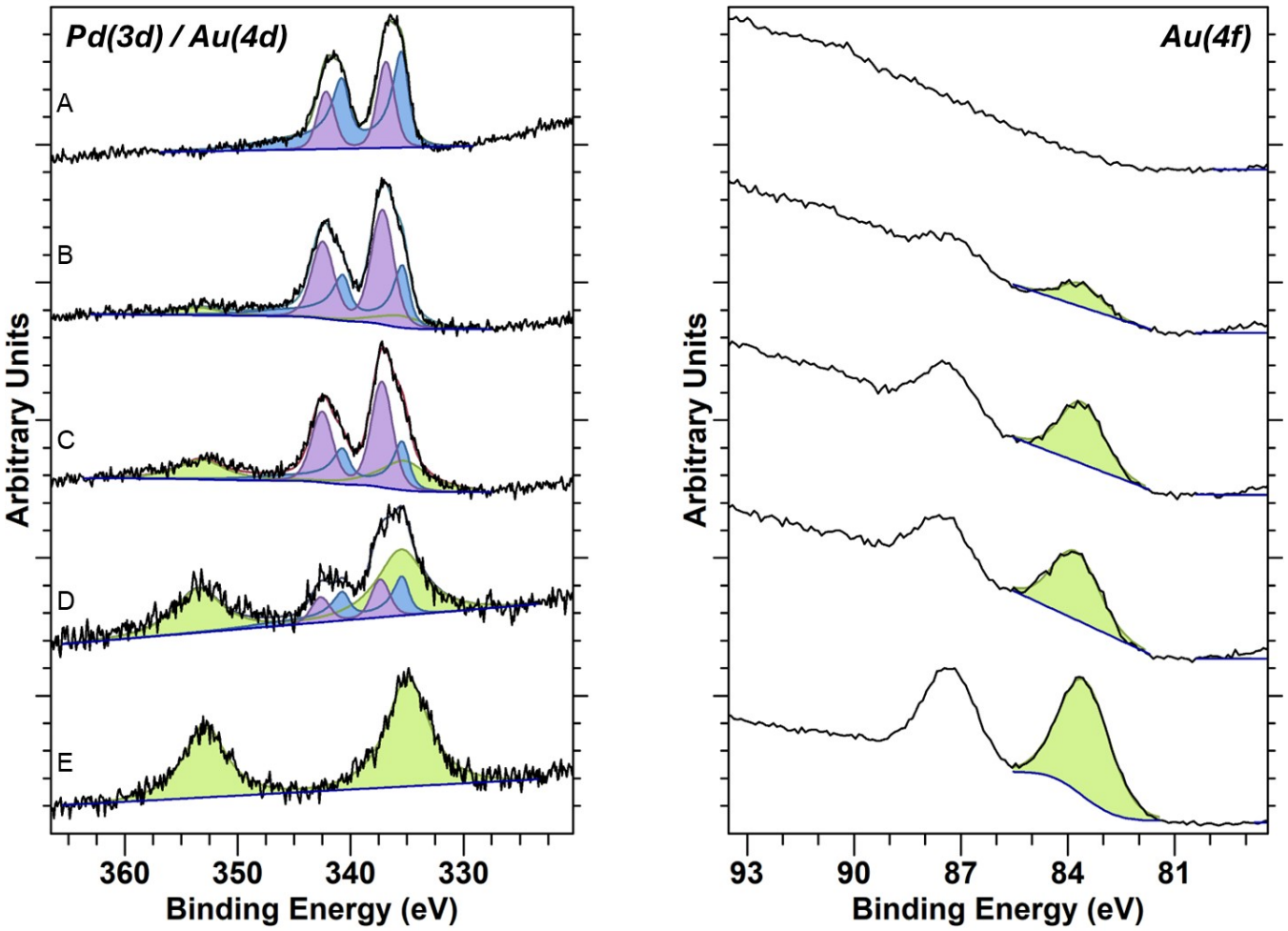

Figure S.3. X-ray photoelectron spectroscopic analysis of the as-prepared **(A)** 1%Pd/Al_2O_3 **(B)** 0.75%Pd-0.25%Au/Al_2O_3, **(C)** 0.5%Pd-0.5%Au/Al_2O_3 **(D)** 0.25%Pd-0.75%Au/Al_2O_3 and **(E)** 1%Au/Al_2O_3 catalysts. ***Key:*** Pd^0 (b*lue*), Pd^{2+} (*purple*), Au (4d) (green). **Note**: All catalysts exposed to a reductive heat treatment (5%H_2/Ar, 4 h, 500 °C, 10 °Cmin^{-1}).

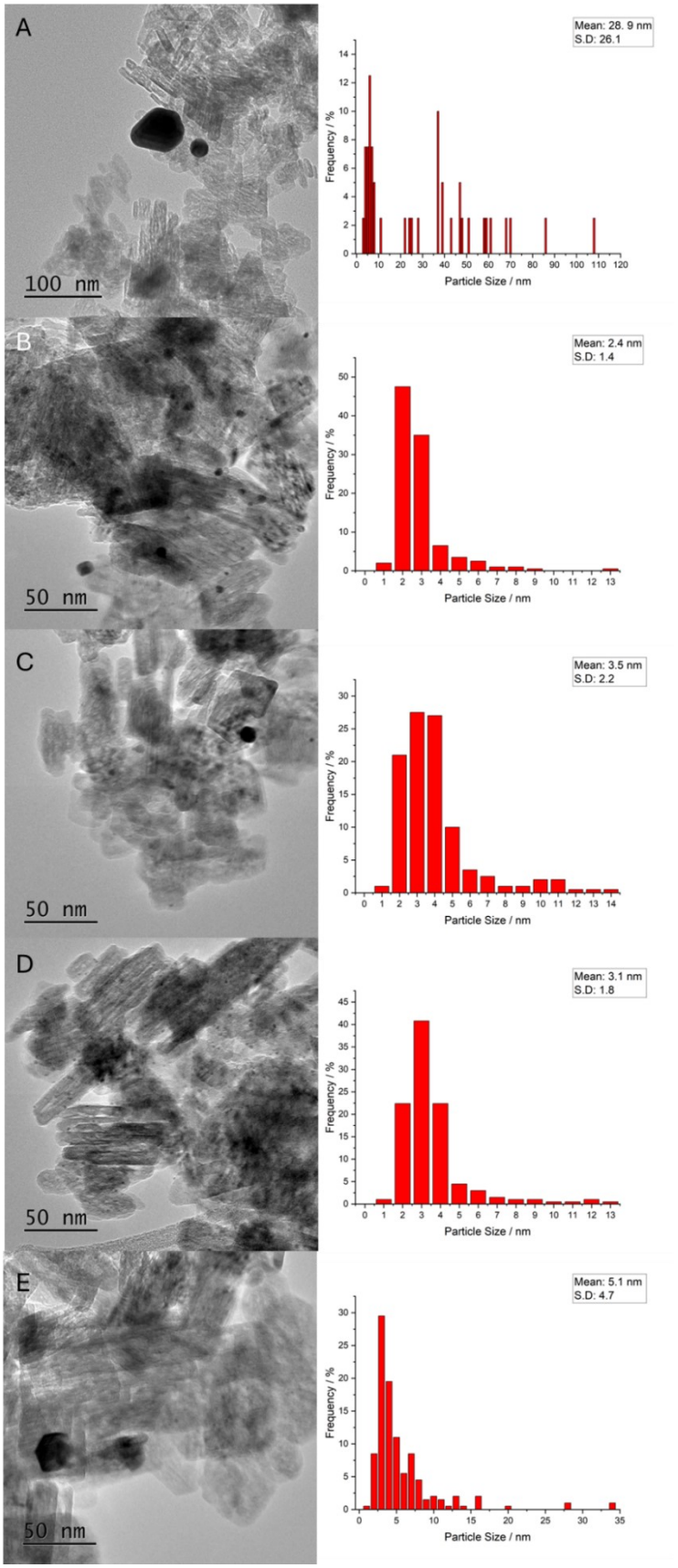

Figure S.4. Representative bright field transmission electron micrographs and corresponding particle size histograms of as-prepared 1%AuPd/Al_2O_3 catalysts **(A)** 1%Au/Al_2O_3 **(B)** 0.75%Au-0.25%Pd/Al_2O_3 **(C)** 0.5%Au-0.5%Pd/Al_2O_3 **(D)** 0.25%Au-0.75%Pd/Al_2O_3 **(E)** 1%Pd/Al_2O_3. **Note**: Catalyst exposed to a reductive heat treatment (5%H_2/Ar, 4 h, 500 °C, 10 °Cmin^{-1}).

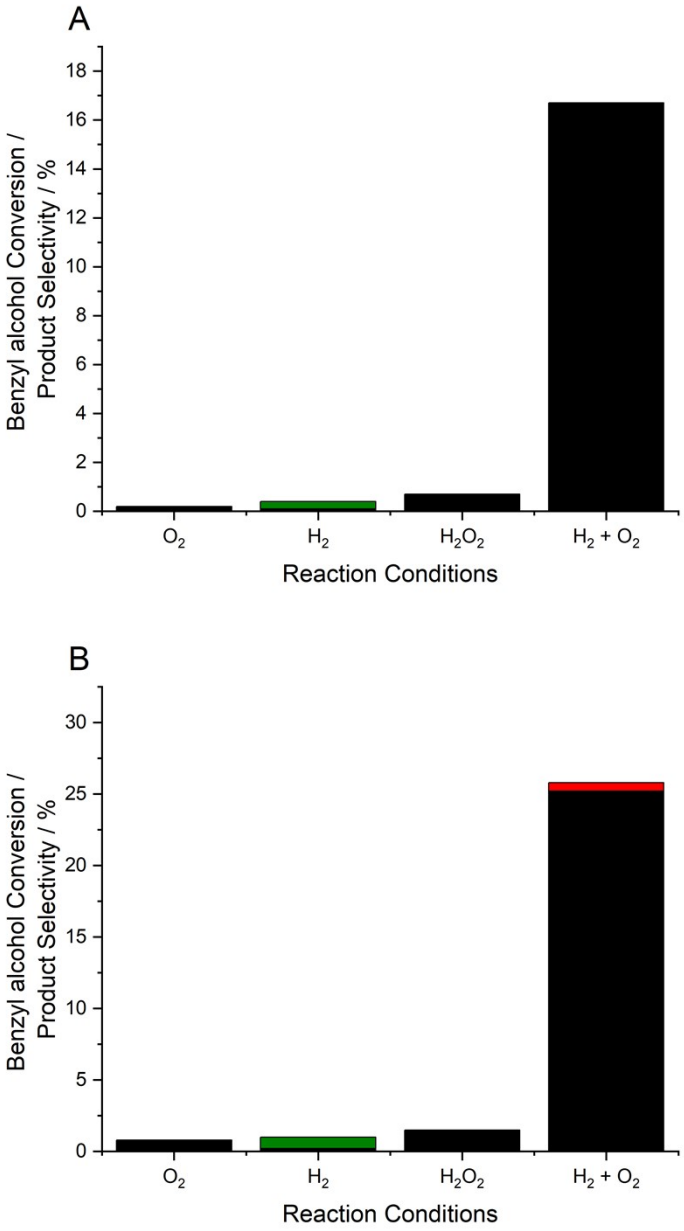

Figure S.5. Catalyst efficacy towards the oxidation of benzyl alcohol as a function of gaseous reagent and H_2O_2 source**. (A)** 1%Pd/Al_2O_3 **(B)** 0.5%Pd-0.5%Au/Al_2O_3 **(C)** 0.5%Pd-0.5%Fe/Al_2O_3 ***Key:*** benzaldehyde (*black bars*) benzoic acid (*red bars*) toluene (*green bars*). **Reaction conditions:** Mass of catalyst (0.01 g), benzyl alcohol (1.04 g, 9.62 mmol), MeOH (7.1 g), 5%H_2/CO_2 (420 psi), 25%O_2/CO_2 (160 psi), 0.5 h, 50 °C, 1200 rpm. **Note 1:** The concentration of commercial H_2O_2 used is comparable to that produced if all H_2 in a standard reaction is converted to H_2O_2. CO_2 in parentheses is indicative of the gaseous atmosphere (580 psi). **Note 2:** For experiments carried out using H_2 or O_2 only, a gaseous mixture of 5%H_2/CO_2 (420 psi) or 25%O_2/CO_2 (150 psi) was used, with the total pressure being maintained at 580 psi using CO_2.

Table S.5.A. Catalytic activity of the 1%Pd/Al_2O_3 catalyst towards the in-situ oxidation of benzyl alcohol, as a function of reaction time.

Reaction time / min	Benzyl alcohol Conv. / %	Benzaldehyde Sel. / %	Benzoic acid Sel. / %	H_2 Conv. / %	H_2 Sel. / %	Residual H_2O_2 / wt.%
15	9.6	100	0	34	69	0.09
30	16.7	100	0	65	63	0.12
45	18.3	100	0	83	54	0.08
60	19.0	100	0	91	51	0.07
90	19.0	100	0	93	50	0.06

In-situ oxidation of benzyl alcohol reaction conditions: Catalyst (0.01 g), benzyl alcohol (1.04 g, 9.62 mmol), MeOH (7.1 g), 5%H_2/CO_2 (420 psi), 25%O_2/CO_2 (160 psi), 50 °C, 1200 rpm. **Note:** H_2 selectivity determined, based on the mol of H_2 utilised in the formation of benzaldehyde.

Table S.5.B. Catalytic activity of the 0.5%Au-0.5%Pd/Al_2O_3 catalyst towards the in-situ oxidation of benzyl alcohol, as a function of reaction time.

Reaction time / min	Benzyl alcohol Conv. / %	Benzaldehyde Sel. / %	Benzoic acid Sel. / %	H_2 Conv. / %	H_2 Sel. / %	Residual H_2O_2 / wt.%
15	14.5	100	0	45	78	0.03
30	22.7	98.2	1.8	71	76	0.04
45	26.1	97.8	2.2	85	73	0.04
60	27.0	97.8	2.2	90	71	0.03
90	27.1	97.4	2.6	93	69	0.01

In-situ oxidation of benzyl alcohol reaction conditions: Catalyst (0.01 g), benzyl alcohol (1.04 g, 9.62 mmol), MeOH (7.1 g), 5%H_2/CO_2 (420 psi), 25%O_2/CO_2 (160 psi), 50 °C, 1200 rpm. **Note:** H_2 selectivity determined, based on the mol of H_2 utilised in the formation of benzaldehyde.

Table S.6. Catalyst stability as a function of reaction time, as determined by ICP analysis of post-in-situ benzyl alcohol oxidation reaction solutions.

	0.5%Au-0.5%Pd/Al_2O_3		1%Pd/Al_2O_3
Reaction time / min	Au / %	Pd / %	Pd / %
15	0.0	0.02	0.06
30	0.0	0.03	0.09
45	0.0	0.05	0.14
60	0.0	0.06	0.21
90	0.0	0.08	0.33

In-situ oxidation of benzyl alcohol reaction conditions: Catalyst (0.01 g), benzyl alcohol (1.04 g, 9.62 mmol), MeOH (7.1 g), 5%H_2/CO_2 (420 psi), 25%O_2/CO_2 (160 psi), 50 °C, 1200 rpm.

Table S.7. Catalytic performance towards the in-situ oxidation of benzyl alcohol over sequential reactions.

Catalyst	Reaction number	Benzyl alcohol Conv. / %	Product distribution / %			Residual H_2O_2 / wt.%
			Benzaldehyde	Benzoic Acid	Toluene	
1%Pd/Al_2O_3	1	16.7	100	0	0	0.12
	2	24.2	98.7	1.3	0	0.11
	3	29.1	98.7	1.3	0	0.11
	4	32.8	98.5	1.5	0	0.10
0.5%Au-0.5%Pd/Al_2O_3	1	22.7	98.2	1.8	0	0.04
	2	39.2	98.2	1.8	0	0.03
	3	49.9	98.4	1.6	0	0.03
	4	62.4	98.4	1.6	0	0.02

In-situ oxidation of benzyl alcohol reaction conditions: Catalyst (0.01 g), benzyl alcohol (1.04 g, 9.62 mmol), MeOH (7.1 g), 5%H_2/CO_2 (420 psi), 25%O_2/CO_2 (160 psi), 50 °C, 1200 rpm.

Table S.8. Comparison of catalytic activity towards the oxidation of benzyl alcohol via in-situ H_2O_2 synthesis.

Catalyst	Solvent	Temperature / °C	Reaction time / h	Benzyl alcohol Conv. / %	Benzaldehyde Sel. / %	H_2 Conv. / %	H_2 Sel. / %	Reaction rate / $mmol_{aldehdyde}mmol_{metal}^{-1}h^{-1}$	Reference
0.8%Pd-0.2%Au/C-H	H_2O	60	6	95.0	90	N.D	N.D	4.0×10^2	3
0.1%Pd@HTS-1-OR	H_2O/MeOH	50	0.5	46.0	100	N.D	N.D	4.54×10^2	4
1.25%Au-1.25%Pd/TS-1	H_2O/MeOH	30	0.5	7.0	93	N.D	N.D	1.65×10^2	5
1%Pd/TiO_2	MeOH	50	0.5	1.8	100	72	9	3.69×10^2	6
0.5%Pd-0.5%Au/TiO_2	MeOH	50	0.5	2.8	100	72	16	7.44×10^2	6
0.5%Pd-0.5%Fe/TiO_2	MeOH	50	0.5	5.8	96	71	33	7.85×10^2	6
2.5%Au-2.5%Pd/TiO_2	MeOH	50	0.5	6.0	90	N.D	N.D	2.81×10^2	7
0.5%Pd-0.5%Au/Al_2O_3	MeOH	50	0.5	11.0	100	50	77	2.92×10^3	8
0.5%Pd-0.5%Fe/Al_2O_3	MeOH	50	0.5	10.3	97	38	92	1.41×10^3	8
1%Pd/Al_2O_3	MeOH	50	0.5	16.7	100	65	63	3.42×10^3	This work
0.5%Pd-0.5%Au/Al_2O_3	MeOH	50	0.5	22.7	98.2	71	76	5.93×10^3	This work

N.D: Not determined.

Catalyst	Solvent	Temp. / °C	Reaction time / h	Oxidant (pressure/psi)	Conv. / %	Benzaldehyde Sel. / %	Rate / $mmol_{aldehyde}/mmol_{metal}/h$	Reference
0.5%Au+0.5%Pd/TiO_2	None	120	0.5	O_2 (150)	61.2	69.2	4.50×10^4	9
0.5%Au+0.5%Pd/C	None	120	0.5	O_2 (150)	81.1	55	4.74×10^4	9
4%Au-0.5%Pd/SBA-15	None	80	2	O_2 (14.7)	20.5	98	9.66×10^0	10
2.5%Au-2.5%Pd/$A_{l2}O_3$	None	100	8	O_2 (29)	83.3	86.6	1.45×10^4	11
2.5%Au-2.5%Pd/TiO_2	None	100	8	O_2 (29)	74.5	91.6	1.37×10^4	11
2.5%Au-2.5%Pd/SiO_2	None	100	8	O_2 (29)	35.7	88	6.29×10^3	11
2.5%Au-2.5%Pd/Fe_2O_3	None	100	8	O_2 (29)	63.4	66.4	8.43×10^3	11
2.5%Au-2.5%Pd/C	None	100	8	O_2 (29)	69.2	46.4	6.43×10^3	11
1% (1Au−3Pd)/CSI	None	120	6	O_2 (150)	94.7	67	1.05×10^3	12
0.33%Au-0.87%Pd/CeO_2	None	160	0.13	O_2 (145)	95	80.7	5.16×10^1	13
1%Pd/Al_2O_3	MeOH	50	0.5	H_2 (21) + O_2 (40)	16.7	100	3.42×10^3	This Work
0.5%Pd-0.5%Au/ Al_2O_3	MeOH	50	0.5	H_2 (21) + O_2 (40)	22.7	98.2	5.93×10^3	This Work

Table S.9. A Comparison of catalytic activity towards the oxidation of benzyl alcohol via aerobic oxidation and in-situ H_2O_2 synthesis.

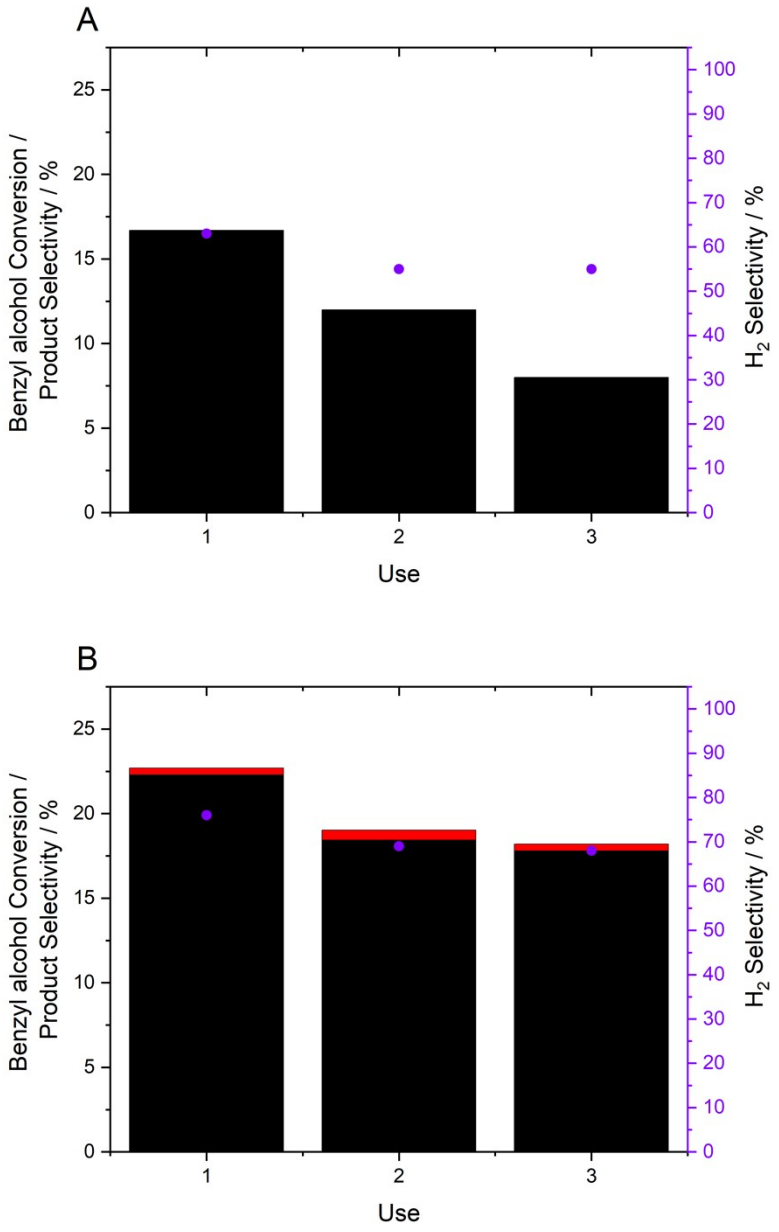

Figure S.6. Comparison of catalytic stability towards the selective oxidation of benzyl alcohol via in-situ H_2O_2 synthesis over the **(A)** 1%Pd/Al_2O_3 and **(B)** 0.5%Au-0.5%Pd/Al_2O_3 catalysts. **Reaction conditions:** Mass of catalyst (0.01 g), benzyl alcohol (1.04 g, 9.62 mmol), MeOH (7.1 g), 5%H_2/CO_2 (420 psi), 25%O_2/CO_2 (160 psi), 50 °C, 1200 rpm. **Note:** H_2 selectivity is determined based on the mol of H_2 utilised in the formation of benzaldehyde.

Table S.10. Catalyst stability over multiple uses in the in-situ benzyl alcohol oxidation reaction, as determined by ICP-MS analysis of post-reaction solutions.

Catalyst	**Metal leached / %**					
	Use 1		**Use 2**		**Use 3**	
	Au	**Pd**	**Au**	**Pd**	**Au**	**Pd**
0.5%Au-0.5%Pd/Al_2O_3	0.0	0.03	0.0	0.08	0.0	0.09
1%Pd/Al_2O_3	N.A	0.09	N.A	0.20	N.A	0.31

Note: data reported is total cumulative metal leaching. N.A = not applicable

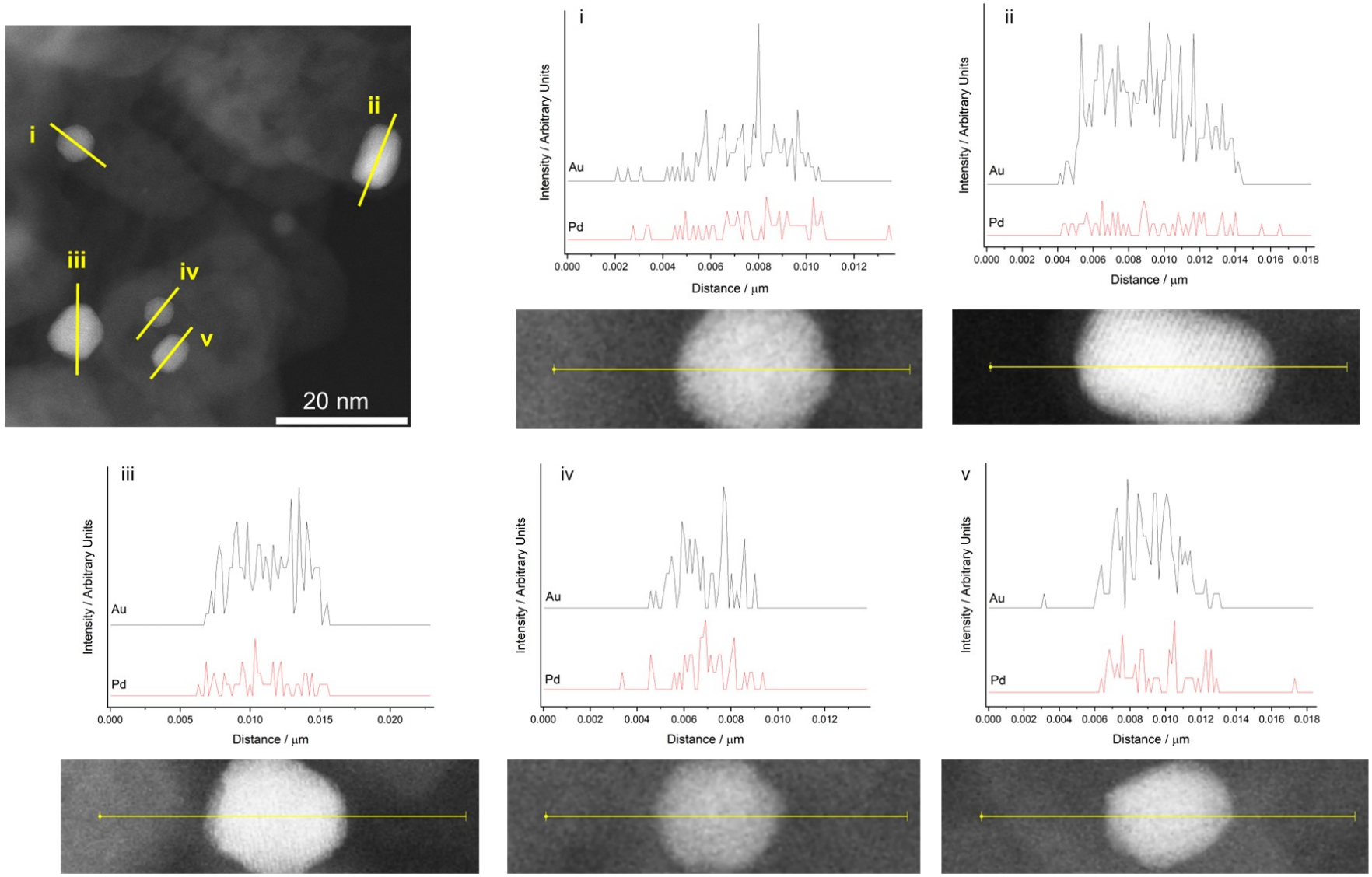

Figure S.7. HAADF-STEM and corresponding XEDS line scan analysis of the indicated nanoparticles showing the presence of both Au (black trace) and Pd (red trace) within the immobilised nanoparticles.

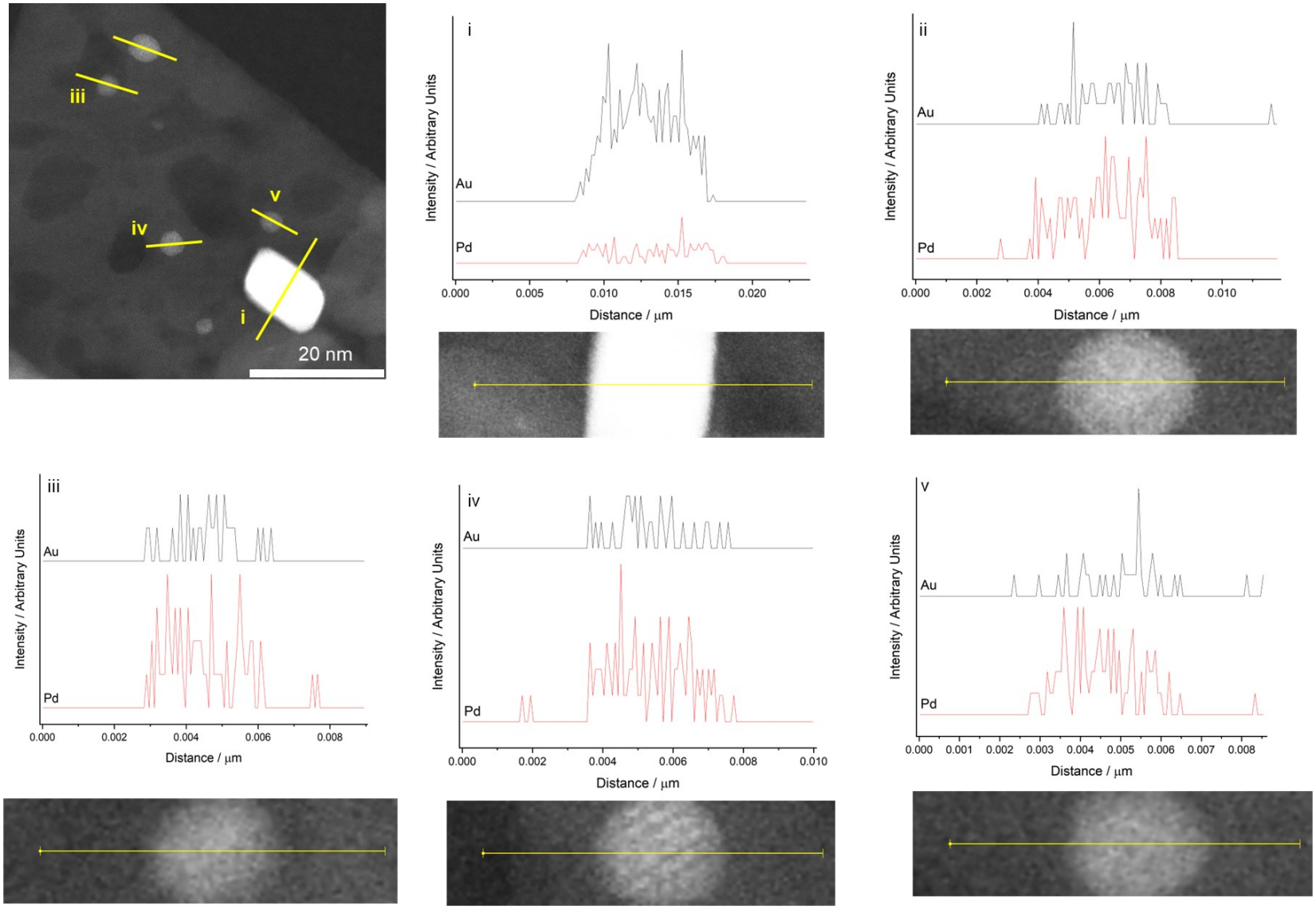

Figure S.8. HAADF-STEM and corresponding XEDS line scan analysis of the indicated nanoparticles showing the presence of both Au(black trace) and Pd (red trace), within the immobilised nanoparticles.

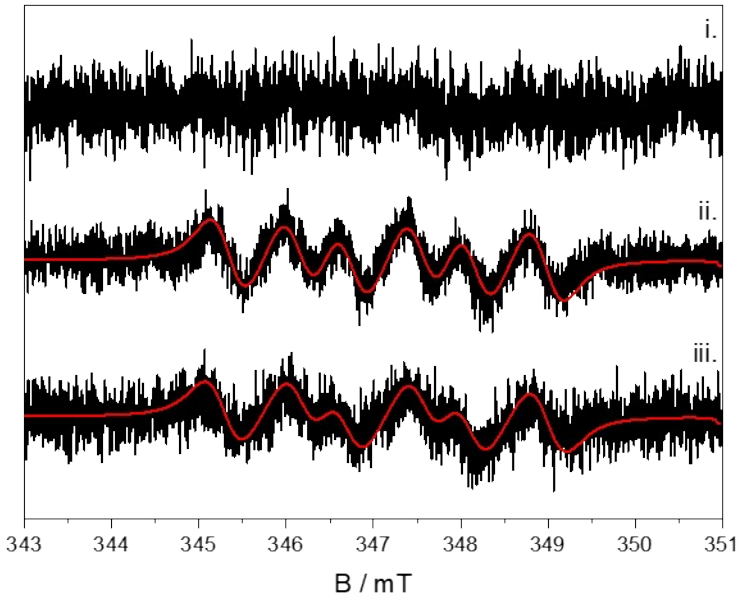

Figure S.9. Control EPR analysis, conducted in methanol over the 0.5%Au-0.5%Pd/Al_2O_3 catalyst, in the presence of DMPO, experimental EPR data reported in black and simulated EPR data reported in red. **(i)** control experiment conducted in the absence of a catalyst showing no signal, **(ii)** control experiment conducted in the absence of gaseous reagents (pressure maintained at 560 psi with CO_2) showing the presence of a DMPO-OCH_3 adduct, **(iii)** control experiment conducted in the absence of benzyl alcohol, showing the presence of a DMPO-OCH_3 adduct. **Reaction conditions:** Mass of catalyst (0.01 g), benzyl alcohol (1.04 g, 9.62 mmol), MeOH (7.1 g), 5%H_2/CO_2 (420 psi), 25%O_2/CO_2 (160 psi), 50 °C, 1200 rpm.

Table S.11. The effect of radical quenchers on the oxidation of benzyl alcohol via in-situ H_2O_2 synthesis over the 0.5%Au-0.5%Pd/Al_2O_3 catalyst.

Quencher	Benzyl alcohol Conv. / %	Benzaldehyde Sel. / %	Benzoic acid Sel. / %
None	22.7	98.2	1.8
Na_2SO_3	9.2	100	0
$NaNO_2$	2.5	100	0

In-situ oxidation of benzyl alcohol reaction conditions: Catalyst (0.01 g), benzyl alcohol (1.04 g, 9.62 mmol), Quencher (0.05 M), MeOH (7.1 g), 5%H_2/CO_2 (420 psi), 25%O_2/CO_2 (160 psi), 50 °C, 1200 rpm.

References.

1. A. R. Wilson, K. Sun, M. Chi, R. M. White, J. M. LeBeau, H. H. Lamb and B. J. Wiley, *J. Phys. Chem. C*, 2013, **117**, 17557-17566.
2. Y. Han, Z. Zhong, K. Ramesh, F. Chen, L. Chen, T. White, Q. Tay, S. N. Yaakub and Z. Wang, *J. Phys. Chem. C*, 2007, **111**, 8410-8413.
3. J. S. Martinez, J. Mazarío, S. Gutiérrez-Tarriño, C. Galdeano-Ruano, J. Gaona-Miguélez, M. E. Domine and P. Oña-Burgos, *Dalton Trans.*, 2022, **51**, 17567-17578.
4. J. Lyu, L. Niu, F. Shen, J. Wei, Y. Xiang, Z. Yu, G. Zhang, C. Ding, Y. Huang and X. Li, *ACS Omega*, 2020, **5**, 16865-16874.
5. I. Moreno, N. F. Dummer, J. K. Edwards, M. Alhumaimess, M. Sankar, R. Sanz, P. Pizarro, D. P. Serrano and G. J. Hutchings, *Catal. Sci.Technol.*, 2013, **3**, 2425-2434.
6. C. M. Crombie, R. J. Lewis, R. L. Taylor, D. J. Morgan, T. E. Davies, A. Folli, D. M. Murphy, J. K. Edwards, J. Qi, H. Jiang, C. J. Kiely, X. Liu, M. S. Skjøth-Rasmussen and G. J. Hutchings, *ACS Catal.*, 2021, **11**, 2701-2714.
7. M. Santonastaso, S. J. Freakley, P. J. Miedziak, G. L. Brett, J. K. Edwards and G. J. Hutchings, *Org. Process Res. Dev.*, 2014, **18**, 1455.
8. G. Sharp, R. J. Lewis, J. Liu, G. Magri, D. J. Morgan, T. E. Davies, Á. López-Martín, R. Li, C. R. Morris, D. M. Murphy, A. Folli, A. I. Dugulan, L. Chen, X. Liu and G. J. Hutchings, *ACS Catal.,* 2024, **14**, 15279-15293.
9. N. Dimitratos, Jose A. Lopez-Sanchez, D. J. Morgan, A. F. Carley, R. Tiruvalam, C. J. Kiely, D/ Bethell and G. J. Hutchings, *Phys. Chem. Chem. Phys.*, 2009, **11**, 5142-5153.
10. C. Y. Ma, B. J. Dou, J. J. Li, J. Cheng, Q. Hu, Z. P. Hao and S. Z. Qiao, *Appl. Catal. B: Environ*. 2009, **92**, 202-208.
11. D. I. Enache, J. K. Edwards, P. Landon, B. Solsona-Espriu, A. F. Carley, A. A. Herzing, M. Watanabe, C. J. Kiely, D. W. Knight, and G. J. Hutchings, *Science*, 2006, **311**, 5759, 362-365.
12. J. Pritchard, L. Kesavan, M. Piccinini, Q. He, R. Tiruvalam, N. Dimitratos, J. A. Lopez-Sanchez, A. F. Carley, J. K. Edwards, C. J. Kiely and G. J. Hutchings, *Langmuir,* 2010, 26, **21**, 16568–16577.
13. H. Zhang, Y. Xie, Z. Sun, R. Tao, C. Huang, Y. Zhao and Z. Liu, *Langmuir* 2011, 27, **3**, 1152–1157.